Electronic-band-structure calculations and soliton dynamics for polyketene and related compounds

Wolfgang Förner and János J. Ladik
Department of Theoretical Chemistry, Friedrich-Alexander-University, Erlangen–Nürnberg, Egerlandstrasse 3, D-8520 Erlangen, Federal Republic of Germany
(Received 23 October 1990; revised manuscript received 17 December 1990)

Recently longer chains of polyketene, which is a variant of *trans*-polyacetylene (*t*-PA) where every second hydrogen atom is substituted by a hydroxyl group, have been synthesized. We performed minimal-basis-set *ab initio* band-structure calculations on polyacetylene and polyketene. In agreement with experimental findings, we found that the fundamental gap of the polymer does not change due to substitution of H by OH. Soliton dynamics within the Su-Schrieffer-Heeger Hamiltonian in polyketene shows a moving soliton in this system, however, with a reduced velocity compared to *t*-PA. Together with our previous results that a C=O group in a *t*-PA chain behaves as a soliton trap and the fact that ≈30% of the CO groups in polyketene are in the keto form instead of the enol form, we can explain the experimental findings of both localized and mobile spins in this material.

I. INTRODUCTION

Solitons are widely used for the interpretation of various experimental results both in physics and chemistry, although the soliton models are frequently questioned. To give at least some examples, let us mention the dynamics of magnetic materials,[1,2] rotations around σ bonds in polymers,[3] and phase changes in solids.[4] An interesting example is the Davydov soliton,[5] which was introduced to explain energy storage and transport in proteins. In the dynamics of the sugar phosphate backbone of deoxyribose nucleic acid (DNA), a soliton was also found.[6] For the explanation of the long-range influence of carcinogens on DNA,[7] a soliton model was suggested and formulated.[8] The dynamics of these solitons have also been studied numerically.[9] A very famous example is the soliton model in *trans*-polyacetylene (*t*-PA) introduced by Su, Schrieffer, and Heeger (SSH).[10] This model gives an explanation for the motional line narrowing in electron paramagnetic resonance spectra and for the spinless charge transport in lightly doped *t*-PA.[10] Simulations of the dynamics of this soliton have been performed for pure *t*-PA (Ref. 11) and also for impurity-containing chains.[12] Since the importance of electron-electron interactions in *t*-PA has been shown,[13] dynamic simulations using the Pariser-Parr-Pople (PPP) model Hamiltonian have also been performed.[14] It was shown that also within PPP theory, a soliton exists in *t*-PA. However, its width is reduced upon inclusion of electron-electron interactions.[14]

Recently a new material, long chains of polyketene, was synthesized.[15,16] According to the experimental data, this material contains rather long segments of the enol form [Fig. 1(a)] interrupted by C=O groups (keto form). Actually, 30% of the material consists of the keto form. The stoichiometry of the material also suggests intramolecular condensation, resulting in a structure as shown in Fig. 1(b).[16] The experimental findings which have to be explained are the following: (i) from uv spectra it is deduced that the optical gap in polyketene is roughly the same as in *t*-PA ($\approx$2 eV) and (ii) in both materials[15,16] there are unpaired spins with a localized (near oxygen) and a mobile fraction.[16] The fact that far fewer unpaired spins are found in the material than in *t*-PA should be due to the ionic polymerization mechanism.[15,16] Upon doping, the conductivity can be changed only by four orders of magnitude, in contrast to *t*-PA. This might be consistent with solitons as charge carriers in the low doping regime, since their concentration in poly- ketene is much smaller than in *t*-PA.

To investigate point (i) (the optical gap) we have performed *ab initio* Hartree-Fock (HF) crystal-orbital[17] cal-

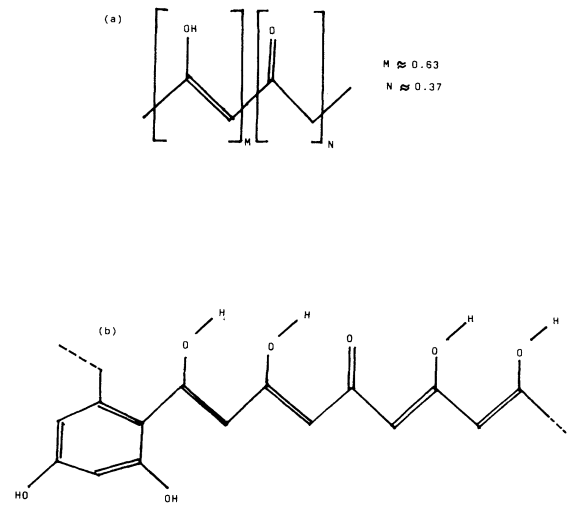

FIG. 1. Suggested structure of polyketene (Ref. 16) without (a) and (b) internal condensation.

culations on *t*-PA and polyketene. To study the soliton properties (ii) we have applied the Su-Schrieffer-Heeger Hamiltonian[10] and performed dynamical simulations.

II. METHOD

The *ab initio* HF crystal-orbital (CO) method used here is well documented in the literature,[17] thus we do not want to elaborate on it here. We used the CO version of the program IBMOL for our calculations.[18] For the geometry of the three compounds considered, we used standard bond lengths and angles, as shown in Fig. 2. The OH groups have been assumed to be in a conformation that allows hydrogen bridging. All two-electron integrals larger than 10^{-8} hartree had been retained. The number of neighbors considered explicitly (strict-neighbor cutoff) was varied. We applied Clementi's minimal (73/21;4/1) (Ref. 19) and double-zeta (95/42;6/2) (Ref. 20) basis sets. The notation (73/21;4/1), e.g., implies that for nonhydrogen atoms (C,O), seven primitive *s*-type Gaussian functions are contracted to two *s*-type atomic orbitals ($1s,2s$) and three sets of primitive Cartesian *p*-type Gaussians are contracted to one set of *p*-type atomic orbitals ($2p$). For hydrogen (and helium), four primitive *s*-type Gaussians are contracted to one *s*-type atomic orbital ("contraction" denotes a linear combination such that the atomic total energy is optimized). The same type of notation is used for the double-zeta basis set. Several studies on the electronic structure of conjugated polymers have shown that for comparative purposes, minimal basis sets can be used safely.[21(a)] For instance, values of band gaps obtained by minimal-basis HF calculations are 6.5 eV for *t*-PA, 8.1 eV for polythiophene (PTP), 8.9 eV for polyfurane (PFU), and 9.1 eV for polypyrrole (PPY).[21(b)] This sequence of calculated band gaps compares qualitatively well with the corresponding sequence of experimental gaps: 1.5 eV (*t*-PA), 2.0 eV (PTP), 2.7 eV (PFU), and 3.0 eV (PPY). This holds as long as the gap values relative to each other are considered. However, for accurate calculations of, e.g., the fundamental band gap, larger basis sets and correlation effects have to be introduced (see Ref. 22 for a recent review).

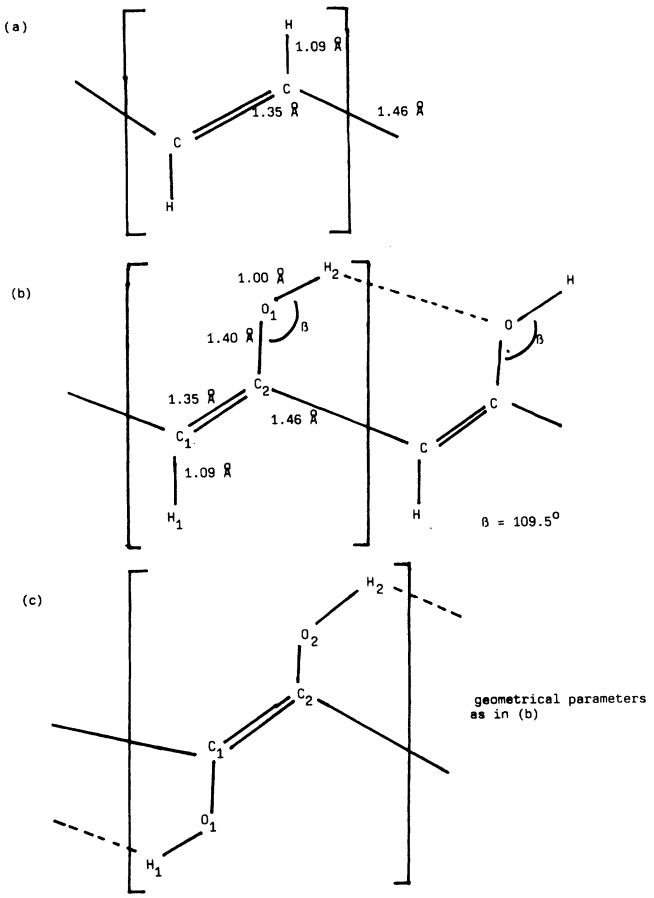

FIG. 2. Geometries for the three compounds considered (all angles are 120° unless otherwise mentioned): (a) *trans*-polyacetylene (*t*-PA); (b) polyketene (PK) in enol form; (c) polydihydroxyacetylene (PDHA).

Our dynamical simulations are based on the SSH model, which is of Hückel type.[10] The CH and C—OH groups are considered as point masses moving in an adiabatically determined potential. Let u_i be the displacement of group i (CH or COH) from its position in the equidistant chain ($u_i=0$). Then for an ideally dimerized (alternating) chain $u_i=(-1)^{i+1}u_0$. The staggered coordinates ψ_i are defined as

$$\psi_i=(-1)^{i+1}u_i \ . \tag{1}$$

Thus in the alternating chain $\psi_i=u_0$ holds. For u_0 we have chosen the experimental value for *t*-PA of 0.03 Å.[23] The soliton manifests itself as the domain wall between dimerization phases A ($\psi_i=u_0$) and B ($\psi_i=-u_0$). From continuum theory we know that the ideal shape of a soliton is[10]

$$\psi_i=-u_0\tanh\left[\frac{i-N_0}{L}\right], \tag{2}$$

where N_0 is the center of the soliton and L is its half-width, which is seven sites in the SSH model of *t*-PA.[10]

The potential in which the groups are moving is given by

$$V=\frac{K}{2}\sum_{i=1}^{N_C-1}(\psi_i+\psi_{i+1})^2 - A\,[\psi_1+(-1)^{N_C}\psi_{N_C}]+E_\pi \ . \tag{3}$$

Here the first term is the harmonic potential between the units, the second one is the linear part of the Taylor series, while E_π is the π-electron energy of the system. K and A are determined such that the predefined equilibrium values of dimerization (u_0) and chain length are a minimum of V.[12] N_C is the number of mobile units in the chain, i.e., the number of carbon atoms. The Hückel matrix for the determinations of E_π consists of two parts:

$$\underline{H}=\underline{H}^{SSH}+\underline{H}' \ . \tag{4}$$

$\underline{H}^{\mathrm{SSH}}$ is the usual SSH Hückel matrix

$$H_{rs}^{\mathrm{SSH}}=\beta_{r,r+1}\delta_{s,r+1}(1-\delta_{rN_C})+\beta_{r,r-1}\delta_{s,r-1}(1-\delta_{r1}) , \tag{5}$$

where ($r,s \le N_C$, all other elements of $\underline{H}$ are zero)

$$\beta_{r,r+1}=-\beta_0+(-1)^r(\psi_r+\psi_{r+1})\alpha . \tag{6}$$

Here $\beta_0=+2.5$ eV and $\alpha=4.1$ eV/Å.[10] Note that Vanderbilt and Mele[24] give a larger value for α (8 eV/Å) and also a larger one for K (about 70 eV/Å^2) on the basis of infrared data. However, with the parameter values of SSH (Ref. 10) at dimerization $u_0=0.03$ Å one obtains reasonable values for band gap and width and K is then determined such that $u_0=0.03$ Å is the equilibrium structure within the model. In $\underline{H}'$ the matrix elements due to the presence of oxygen are included:

$$H'_{rs}=I_r\delta_{rs}+\beta_{\mathrm{C\text{-}O}}\Omega_{rs} . \tag{7}$$

Here[24]

$$I_r=\begin{cases}0 & \text{if } r \text{ corresponds to a CH site}\\ -0.1\,\beta_0 & \text{if } r \text{ corresponds to C of a COH site}\\ -2.0\,\beta_0 & \text{if } r \text{ corresponds to O of a COH site .}\end{cases} \tag{8}$$

$\beta_{\mathrm{C\text{-}O}}=-0.85\beta_0$ (Ref. 25) and Ω_{rs} is equal to 1 if r and s correspond to a C—O bond and are 0 otherwise. Thus $\underline{H}$ has the dimension $N\times N$ with $N=N_C+N_O$, where N_O is the number of oxygen atoms and N_C the number of CH and COH units together.

Diagonalization of $\underline{H}$,

$$\underline{H}\mathbf{c}_i=\varepsilon_i\mathbf{c}_i , \tag{9}$$

yields the eigenvalues (ε_i) and eigenvectors ($\mathbf{c}_i$) and thus the charge-density bond-order matrix is

$$P_{rs}=\sum_{i=1}^{N}(O_i^{\alpha}+O_i^{\beta})c_{ri}c_{si} \tag{10}$$

(O_i^{γ} is the occupation number of the ith orbital for spin γ) and the total π-electron energy is

$$E_{\pi}=\sum_{r,s}P_{rs}H_{rs}=\sum_{i=1}^{N}(O_i^{\alpha}+O_i^{\beta})\varepsilon_i . \tag{11}$$

The dynamics of the system can be obtained by[26]

$$m_i\ddot{\psi}_i=-\frac{\partial V}{\partial\psi_i}\quad(i\le N_C) , \tag{12}$$

where m_i are the masses of the CH or COH units. The gradients of E_π occurring in[12] are computed exactly:[27]

$$\frac{\partial E_\pi}{\partial\psi_i}=\sum_{r,s}\left[\frac{\partial H_{rs}}{\partial\psi_i}P_{rs}+H_{rs}\frac{\partial P_{rs}}{\partial\psi_i}\right] . \tag{13}$$

This is made possible by the fact[27] that

$$\sum_{r,s}H_{rs}\frac{\partial P_{rs}}{\partial\psi_i}=0 . \tag{14}$$

Analytical calculation of $\partial H_{rs}/\partial\psi_i$ is trivial. For computation of the dynamics we used the algorithm applied by Su and Schrieffer[26] ($\omega_i=\dot{\psi}_i$):

$$\omega_i(t+\tau)=\omega_i(t)-\tau\frac{\partial V(t)}{\partial\psi_i}\Big/m_i ,$$
$$\psi_i(t+\tau)=\psi_i(t)+\tau\omega_i(t+\tau) . \tag{15}$$

The time step τ was chosen as 1 fs, which guarantees a sufficiently constant total energy. As starting configurations for our soliton simulations we used the end-kink geometries shown in Fig. 3.

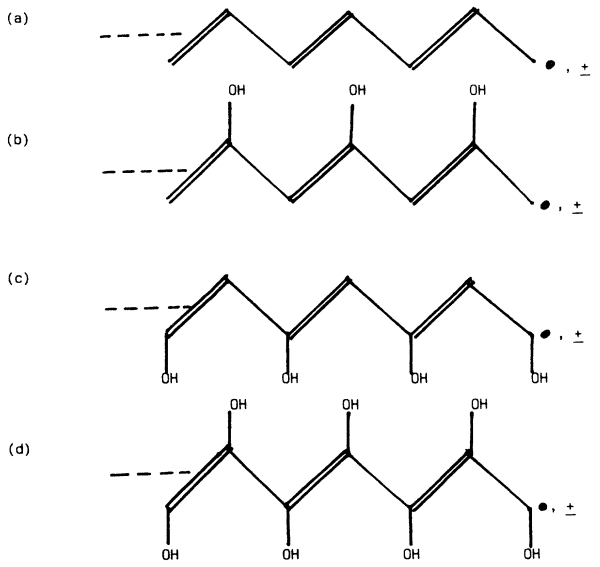

FIG. 3. End-kink configurations (where the soliton is initially localized at the unsaturated carbon in the terminal long bond of the chain) used in our simulations as start at $t=0$ (●, +, − stand for neutral, positively, and negatively charged kinks, respectively): (a) all-*trans*-polyacetylene; (b),(c) polyketene with the two topologically different kink positions; (d) polydihydroxyacetylene.

III. RESULTS AND DISCUSSION

A. Band-structure calculations

In Table I we show the net charge distribution obtained by Mulliken population analysis[28] for the three compounds under study: polyacetylene (*t*-PA), polyketene (PK), and polydihydroxyacetylene (PDHA), where *t*-PA and PK chains are experimentally known. Obviously, in the case of the minimal basis (MB) set, calculations on *t*-PA and PK the charge distributions are sufficiently converged in the third-neighbor calculations. Thus PDHA was computed only in this approximation, and also double-zeta (DZ) basis-set calculations have been performed only for this case. In case of the DZ basis, the oxygen atom is more electronegative than in the minimal basis. The net negative charge on oxygen increases by $\approx 0.1e$, while the negative charge on the carbon not attached to oxygen decreases by nearly the same amount. Table II gives some details of the band structures of our systems. Again it is obvious that all quantities shown (total energy, band gap, and widths of valence and conduction bands) are sufficiently converged in the third-neighbor interaction approximation. However, their limits are still not fully converged. There is no big difference between *t*-PA and PK, as one can see from Table II. In both cases, the upper limit of the valence band is about -9 eV in minimal basis. In PDHA the valence band is shifted upward by roughly 1 eV. However, the width of the valence band reduces from 7.4 eV (*t*-PA) to 5.6 eV (PK) and further to 5.1 eV (PDHA). The conduction band is shifted upward from -1.7 eV (*t*-PA) to -1.2 eV (PK) and does not change anymore in going to PDHA. Its width changes between 8.8 and 9.3 eV in the three polymers. The fundamental gap increases from 7.15 eV in *t*-PA by ≈ 0.2 eV to 7.37 eV in PK. The DZ basis reduces both gaps by 0.4–0.5 eV, and their difference is increased to ≈ 0.3 eV.

Although the absolute values of the gap in MB or DZ calculations are certainly not realistic, the qualitative result that *t*-PA and PK should show roughly the same fundamental band-gap values should be correct. This finding agrees with experiment,[15,16] which shows a gap of ≈ 2 eV in both polymers. As demonstrated clearly in papers by Suhai[29] and Liegener[30] on *t*-PA the inclusion of electronic correlations at least on the level of Møller-Plesset (MP) many-body perturbation theory in second or third order is of utmost importance to obtain agreement with experiment for the gap, which can be corrected using the electronic polaron concept (see also Ref. 22 for a recent review). It is shown[30] that in the Hartree-Fock limit (gap value converged with respect to the size of the basis set) the gap of *t*-PA is ≈ 6.2 eV, which is reduced to ≈ 1.8 eV on MP2 and again increased to ≈ 2.0 eV on the MP3 level. The shoulder around 1.5 eV in the spectrum of *t*-PA might be due to excitonic transitions.[30] However, the theoretical exciton binding energy of ≈ 1.4 eV (Ref. 30) would then be somewhat too large, probably due to the neglected lattice-relaxation effects. From a qualitative point of view, one can argue that the interaction of the filled-π lone pair of oxygen with the π,π^* orbitals of the backbone results in first-order perturbation theory (on the Hückel level) in a constant shift of both backbone orbitals, which does not change the gap. In PDHA, however, the gap is reduced to 6.56 eV already in the MB calculation. Thus the presence of OH groups at all carbons seems to affect the backbone stronger than an OH group at every second carbon.

Finally, in Fig. 4 we show the valence- and conduction-band regions of the three polymers. Comparing the valence-band regions of *t*-PA [Fig. 4(a)] and PK [Fig. 4(b)] one sees that the valence band (π) is somewhat compressed in PK, but its upper limit is not changed too much. This is easy to understand. The interaction of the π band with the oxygen lone pair (O $2p$) shifts the π band upwards, but does so in its lower region more strongly than in the upper region, as expected, due to the smaller energy separations between the bands in the lower region of the valence band. Note that the lone-pair band lies mostly below the valence band. For the bands 1–3 the same holds, but their forms are not changed too much. However, in PK the three bands are crossed by the band

TABLE I. Net charge distributions of the three compounds studied as functions of the number of neighbors (N) taken into account and of the basis set applied (the asterisk denotes the DZ basis, all other results are in the minimal basis).

	$(C_2H_2)_x$	$(C_2HOH)_x$				
N	$C(q_H=-q_C)$	H_1	C_1	C_2	O_2	H_2
1	−0.211	0.211	−0.267	0.176	−0.573	0.454
2	−0.210	0.212	−0.283	0.190	−0.582	0.463
3	−0.210	0.212	−0.295	0.201	−0.585	0.466
3*	−0.164	0.186	−0.205	0.260	−0.687	0.446
4	−0.210	0.212	−0.300	0.206	−0.586	0.468
5	−0.209	0.212	−0.303	0.209	−0.586	0.469
6	−0.209	0.212	−0.305	0.211	−0.587	0.469
			$[C_2(OH)_2]_x$			
	H_1	O_1	C_1	C_2	O_2	H_2
3	0.469	−0.589	0.120	0.122	−0.589	0.466

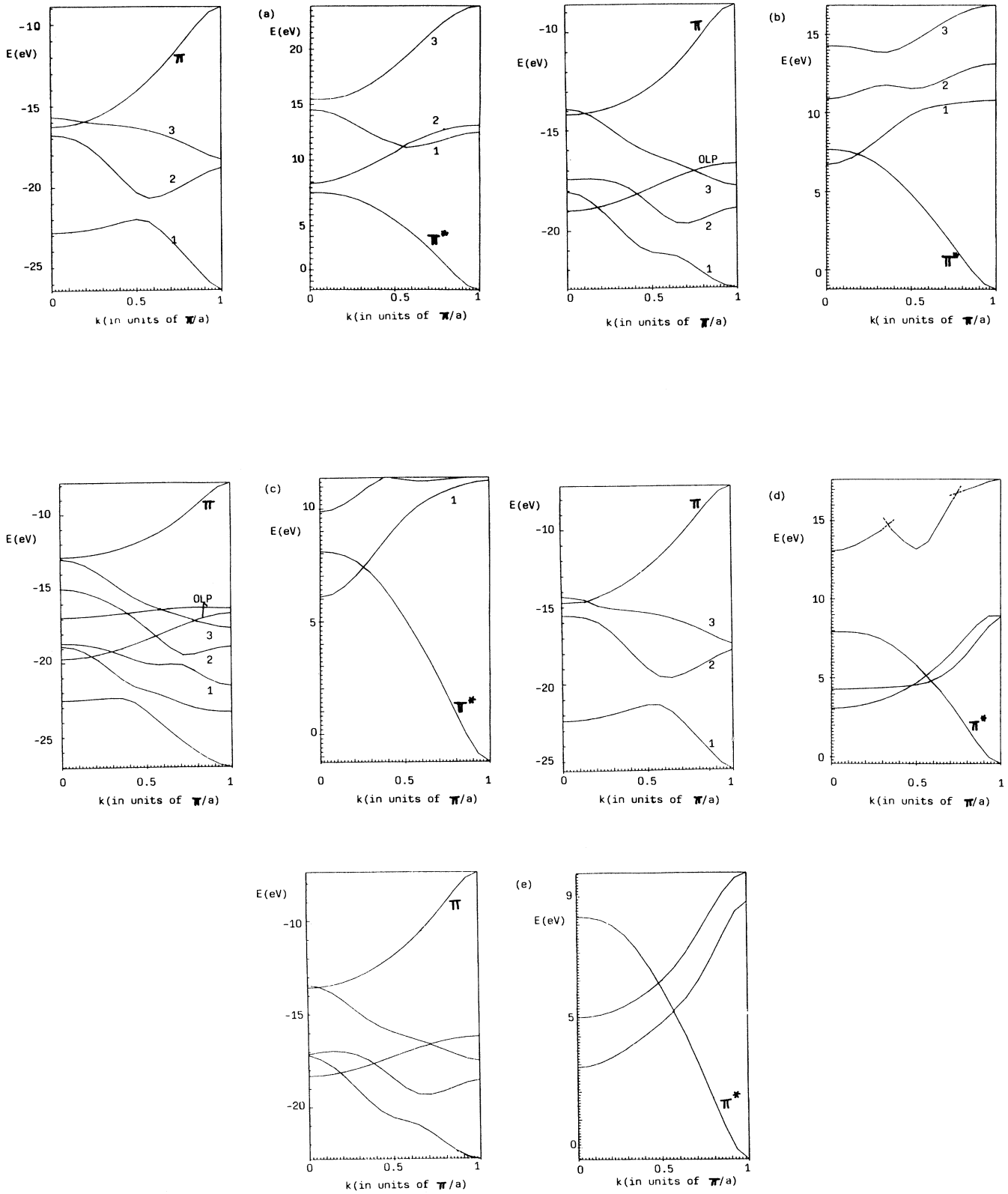

FIG. 4. Valence- and conduction-band regions for the three compounds studied (OLP denotes oxygen lone pair): (a) $(C_2H_2)_x$, third-neighbor interactions, MB; (b) $(CHCOH)_x$, third-neighbor interactions, MB; (c) $[C_2(OH)_2]_x$, third-neighbor interactions, MB; (d) $(C_2H_2)_x$, third-neighbor interactions, DZ; (e) $(CHCOH)_x$, third-neighbor interactions, DZ.

TABLE II. Total energy (E_t), upper limit and width of the valence band (v), and lower limit and width of the conduction band (c) for the three compounds studied as functions of the number of neighbors (N) taken into account and of the basis set (the asterisk denotes the DZ basis, all other results are in the minimal basis).

			Valence band		Conduction band	
	E_t (eV)[a]	E_g (eV)	Upper limit (eV)	width (eV)	Lower limit (eV)	width (eV)
N	(E_t+2083 eV)			$(CH_2)_x$		
1	−0.671	6.06	−9.30	8.08	−3.25	8.79
2	−1.084	7.07	−9.03	7.41	−1.96	9.06
3	−1.096	7.15	−8.89	7.39	−1.74	8.80
3*	−8.110	6.67	−7.09	7.63	−0.42	8.36
4	−1.095	7.19	−8.81	7.36	−1.62	8.84
5	−1.094	7.22	−8.76	7.35	−1.54	8.79
6	−1.094	7.23	−8.72	7.34	−1.49	8.80
	(E_t+4115 eV)			$(CHCOH)_x$		
1	−0.096	6.56	−9.07	6.06	−2.51	8.70
2	−0.512	7.32	−8.74	5.59	−1.43	9.06
3	−0.535	7.37	−8.60	5.59	−1.23	8.87
3*	−12.127	6.96	−7.40	6.16	−0.44	8.71
4	−0.540	7.41	−8.52	5.57	−1.11	8.90
5	−0.541	7.43	−8.46	5.56	−1.03	8.86
6	−0.542	7.45	−8.42	5.55	−0.97	8.86
	(E_t+6146 eV)			$[C_2(OH)_2]_x$		
3	−0.607	6.56	−7.81	5.08	−1.25	9.33

[a]Since the total energy in eV is a large number, we added to all E_t values in the corresponding part of the table the indicated number (E_t + number) to make the effects of N and of the basis set more clearly visible.

corresponding to the oxygen long pair. The conduction band does not change too much due to the OH groups. However, its lower limit is somewhat more shifted up than the upper limit of the valence band, resulting in a small increase of the gap. Comparison with the corresponding DZ band structures [Figs. 4(d) and 4(e)] shows that the better basis set results in a shift of the conduction-band region to lower energies. The overall forms and relative positions of the bands are not changed too much. In the conduction-band regions, the band structures become more complicated due to band crossings.

In the case of PDHA [Fig. 4(c)] we can identify again the bands π and 1–3 in the valence-band region. However, now 1–3 are crossed by two oxygen lone-pair bands. The conduction-band region is not changed too much. However, due to the interaction with two oxygen lone-pair orbitals, the upper limit of the valence band is pushed up more than in PK, resulting in a considerable decrease of the gap.

B. Soliton properties

Besides performing dynamical simulations, we have also optimized the soliton half-width L, determined the dimerization energy, which is the difference of energy between alternating (alternating long and short bonds, dimerized system, $\psi_i = u_0$), and equidistant (all bonds of equal length, metallic system, $\psi_i = 0$) chains, the energy difference between an optimized soliton in the middle of the chain and the equidistant chain (E_L-E_0), and the energy difference between a soliton in the middle of the chain and the end-kink configuration (E_L-E_1). These quantities are collected, together with spring constants (K) and soliton velocities (v_s) for different chains in Table III. Let us first concentrate on the neutral solitons in the different chains ($N = 31$, 51, and 71). In all three cases the alternating chain (with a kink at the chain end) is more stable than the equidistant one (E_{Dim}), and an optimized soliton in the middle of the chain (E_L-E_0) is further stabilized (compared to the end kink) by roughly 1 eV. The same holds for the OH-containing groups and the charged chains. These quantities increase naturally with the chain length and diverge for $N \to \infty$. However, E_L-E_1 should converge to a constant value for $N \to \infty$. It corresponds to the maximal energy a soliton can carry, starting from an end kink. We find −0.891 eV for $N = 31$, −0.922 eV for $N = 51$, and −0.935 eV for $N = 71$. We have found similar values for oxygen-containing chains. The energy values do not change with charge, since the electrons are added to (removed from) the soliton level, which has an energy of zero (midgap) in the Hückel case by symmetry. Another converging quantity is the spring constant (K) for which we find 19.318

TABLE III. Dimerization energy (E_{Dim}), optimum soliton width (L), energy difference (E_L-E_0) for a soliton in the middle of an alternating chain and an equidistant chain, energy difference (E_L-E_1) for a soliton in the middle of a chain and an end-kink geometry, spring constant K of a chain, and soliton velocity (v_s) for chains of different lengths (N), charge (C) at the carbon atoms, and for different positions of OH groups (no OH groups, OH at odd-numbered carbons only, OH at even-numbered carbons only, and OH at all carbons).

N	C($\|e\|$)	OH	E_{Dim} (eV)	L	E_L-E_0 (eV)	E_L-E_1 (eV)	K (eV/Å^2)	v_S (km/s)
31	0	no	0.145	4	−1.036	−0.891	19.318	75.8
		odd	0.123	4	−0.962	−0.839	18.202	60.6
		even	0.123	4	−0.962	−0.839	18.202	60.6
51	0	no	0.343	5	−1.265	−0.922	20.217	82.8
		odd	0.278	5	−1.144	−0.866	18.990	66.3
		even	0.278	5	−1.144	−0.866	18.990	66.3
		all	0.298	5	−1.135	−0.837	18.361	27.6
51	+1	no	0.343	5	−1.265	−0.922	20.217	86.4
		odd	0.278	5	−1.144	−0.866	18.990	71.0
		even	0.278	5	−1.144	−0.866	18.990	71.0
		all	0.298	5	−1.135	−0.837	18.361	27.6
51	−1	no	0.343	5	−1.265	−0.922	20.217	86.4
		odd	0.278	5	−1.144	−0.866	18.990	71.0
		even	0.278	5	−1.144	−0.866	18.990	71.0
		all	0.298	5	−1.135	−0.837	18.361	27.6
71	0	no	0.558	6	−1.493	−0.935	20.603	82.2
		odd	0.440	6	−1.316	−0.877	19.329	67.2
		even	0.440	6	−1.316	−0.877	19.329	67.2

eV/Å^2 ($N=31$), 20.217 eV/Å^2 ($N=51$), and 20.603 eV/Å^2 ($N=71$). However, as expected from previous work,[31] the soliton half-width L converges very slowly from $L=4$ ($N=31$) to $L=6$ ($N=71$). For $N\rightarrow\infty$, $L\approx 7$ is the width in the SSH case.[10,26] Interestingly, L does not change at all upon the addition of OH groups.

For $N=71$ we show some soliton properties in neutral chains in Fig. 5. Without any OH groups, in Fig. 5(a) we see the usual spin distribution of a soliton ($L=6$) in the middle of the chain. Obviously, the spin distribution extends further from the soliton center than the lattice distortion. From Fig. 5(a) one can deduce that the energy of an optimized ($L=6$) soliton at the chain end is roughly 0.5 eV compared to its equilibrium position. The energy E_L-E_1 in Table III is the energy of an end kink (ideally dimerized chain) and not of a soliton of six-lattice-site width and is thus larger. The energy of the soliton as function of its position in the chain ($L=6$) shows that obviously between units 25 and 45 (note that the curve extends symmetrically to the displayed part from sites 36–71) the soliton can move freely without loss of energy. Since the Hückel-type model Hamiltonian is spin independent, it cannot describe the experimentally observed spin polarization in the material. Figure 5(b) shows the spin and charge distribution in a chain with OH groups at odd-numbered carbons. Obviously, a fraction of the spin density is now located at the oxygens (stars). We see that the negative charge is mainly located at even-numbered carbons (dashed line), however, in a rather uniform manner, while at odd-numbered carbons (solid line) we find a solitonlike structure in the charge distribution. The oxygens (stars) carry uniformly a positive charge, since they are π donors (and σ acceptors). If the oxygens are attached at even-numbered carbons, they carry no spin [Fig. 5(c)], and now the major contribution of negative charge is carried by the odd-numbered carbons. If OH groups are attached to each carbon, we see that the spin and charge distributions [Fig. 5(d)] are combinations of those discussed above.

From Table III we see that the velocities of neutral solitons converge from 75.7 km/s ($N=31$) via 82.8 km/s ($N=51$) to 82.2 km/s ($N=71$). If OH groups are attached to every second carbon, v_s is reduced from 82.8 to 66.3 km/s for $N=51$. To which sites the OH are attached (odd or even) plays no role in this case. If OH groups are attached to all carbons, the soliton velocity is reduced drastically to 27.6 km/s.

The time evolutions of the spin density at odd-numbered carbons are shown in Fig. 6. From comparison of Fig. 6(b) with Fig. 6(c) we see that the spin-density fraction at oxygen (attached to odd-numbered carbons) follows the soliton. The same holds if the OH group is attached to all carbons [Figs. 6(e) and 6(f)]. If OH is attached at even-numbered carbons, the oxygens carry no spin.

If we turn to negatively charged solitons, we see from Table III that charged solitons are by $\approx$4–5 km/s faster than neutral ones (in the cases of t-PA and PK). Positively charged solitons behave identically to negatively charged ones. In Fig. 7(a) we see the usual charge distri-

bution of a negatively charged solition in a t-PA chain. Figure 7(b) shows the distribution for a chain with OH at odd-numbered carbons. Similarly to the spin distribution in neutral solitons, we find a soliton structure for odd-numbered carbons and oxygens; however, the oxygens are positively charged. The even-numbered carbons show a rather uniform charge distribution. If the OH groups are attached to even-numbered carbons [Fig. 7(c)] the charge at the oxygens becomes uniform, as expected. With OH groups at every carbon [Fig. 7(d)] we find again a kind of superposition of Figs. 7(b) and 7(c). Finally, in Fig. 8 we show the time evolution of the charge distribution for a negatively charged end kink. The results are rather similar to neutral solitons. Thus in chains with OH groups attached we find solitons with properties similar to the corresponding ones in t-PA. Only quantitative changes in the velocities are found. The wiggles in the charge-density evolutions, especially in Figs. 8(b) and 8(c), are due to the influence of the oxygen atoms (which are located only at every second carbon) on the corresponding carbon atoms. In addition, phonons also influence the charge-density evolutions.

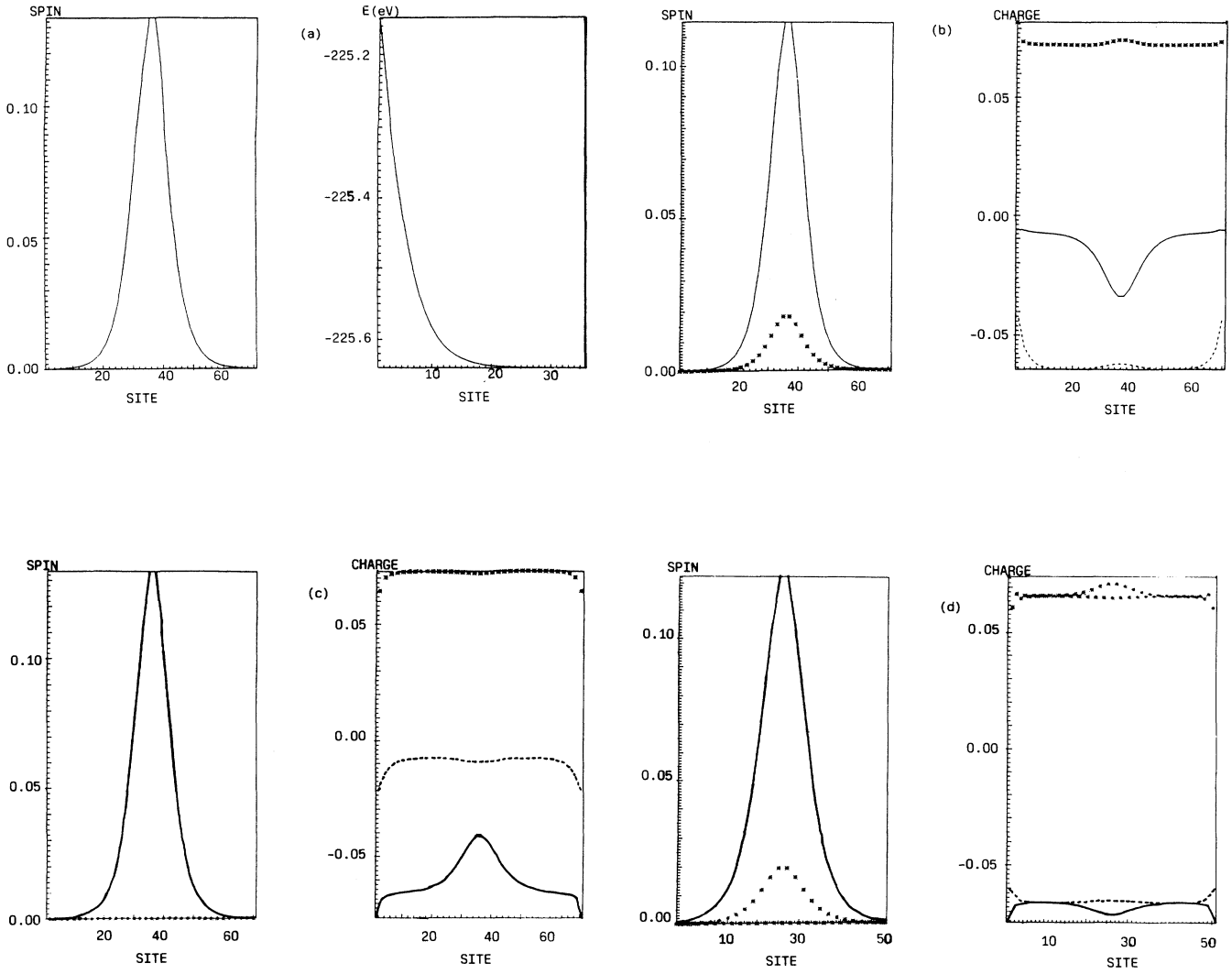

FIG. 5. Different soliton properties in neutral $N=71$ chains. (a) Spin density for an optimized soliton in the middle of the chain and its energy as function of its position. (b) Spin and charge distribution for an optimized soliton in the middle of the chain with OH groups at the odd-numbered carbons (solid lines, odd-numbered carbons; dashed lines, even-numbered carbons; stars, oxygen). (c) Same as (b), but with OH groups at even-numbered carbons. (d) Same as (b) but with OH groups at all carbons and $N=51$.

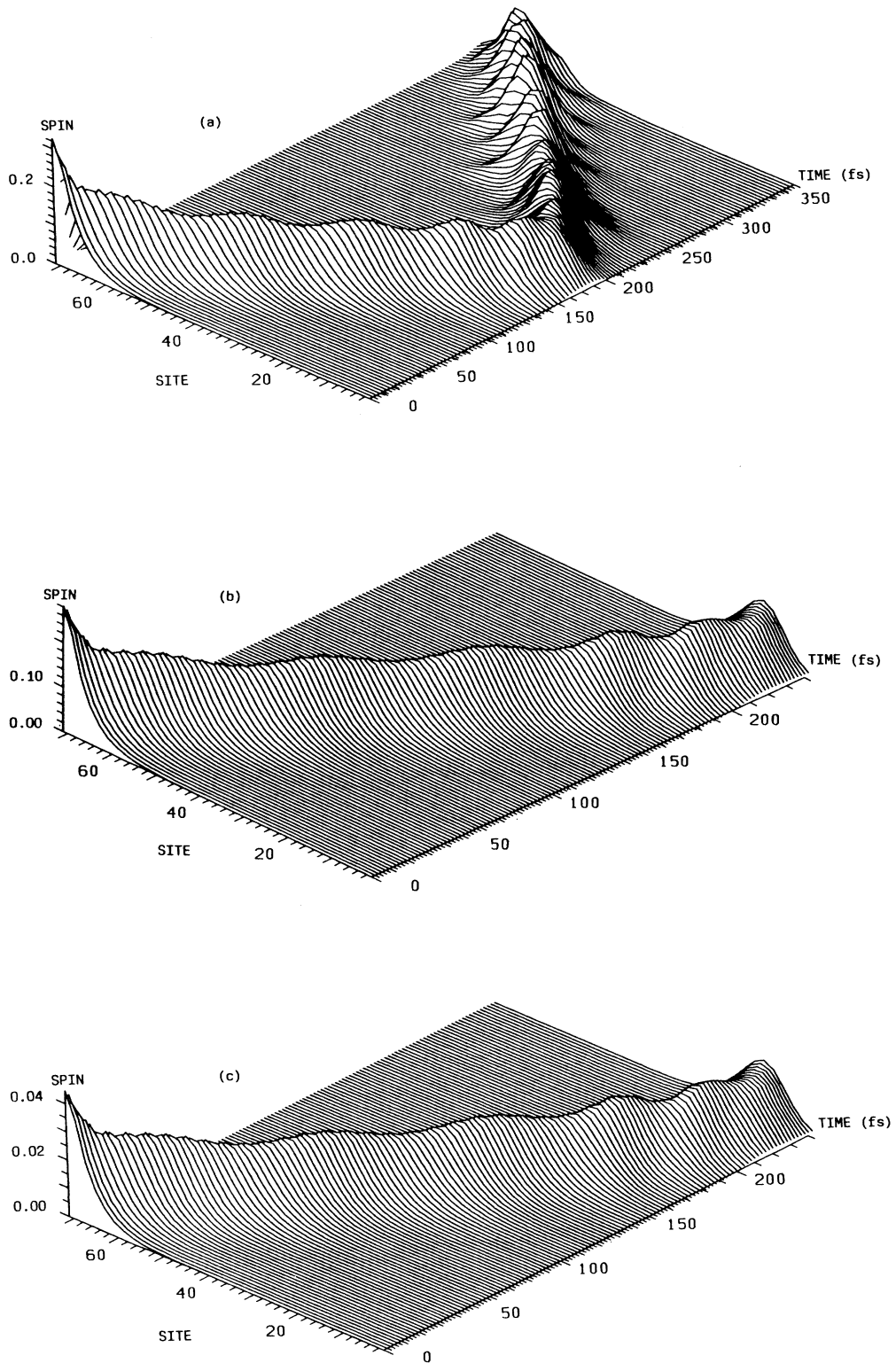

FIG. 6. Evolution of the local spin density (ρ_k) at odd-numbered carbons as function of site (k) and time t (in fs) in a neutral chain of 71 units starting from an end-kink geometry. (a) No OH groups; (b) OH groups at odd-numbered carbons; (c) same as (b) but spin densities at the oxygens; (d) OH groups at even-numbered carbons; (e) OH groups at all carbons, but $N=51$; (f) same as (e) but spin densities at the oxygens.

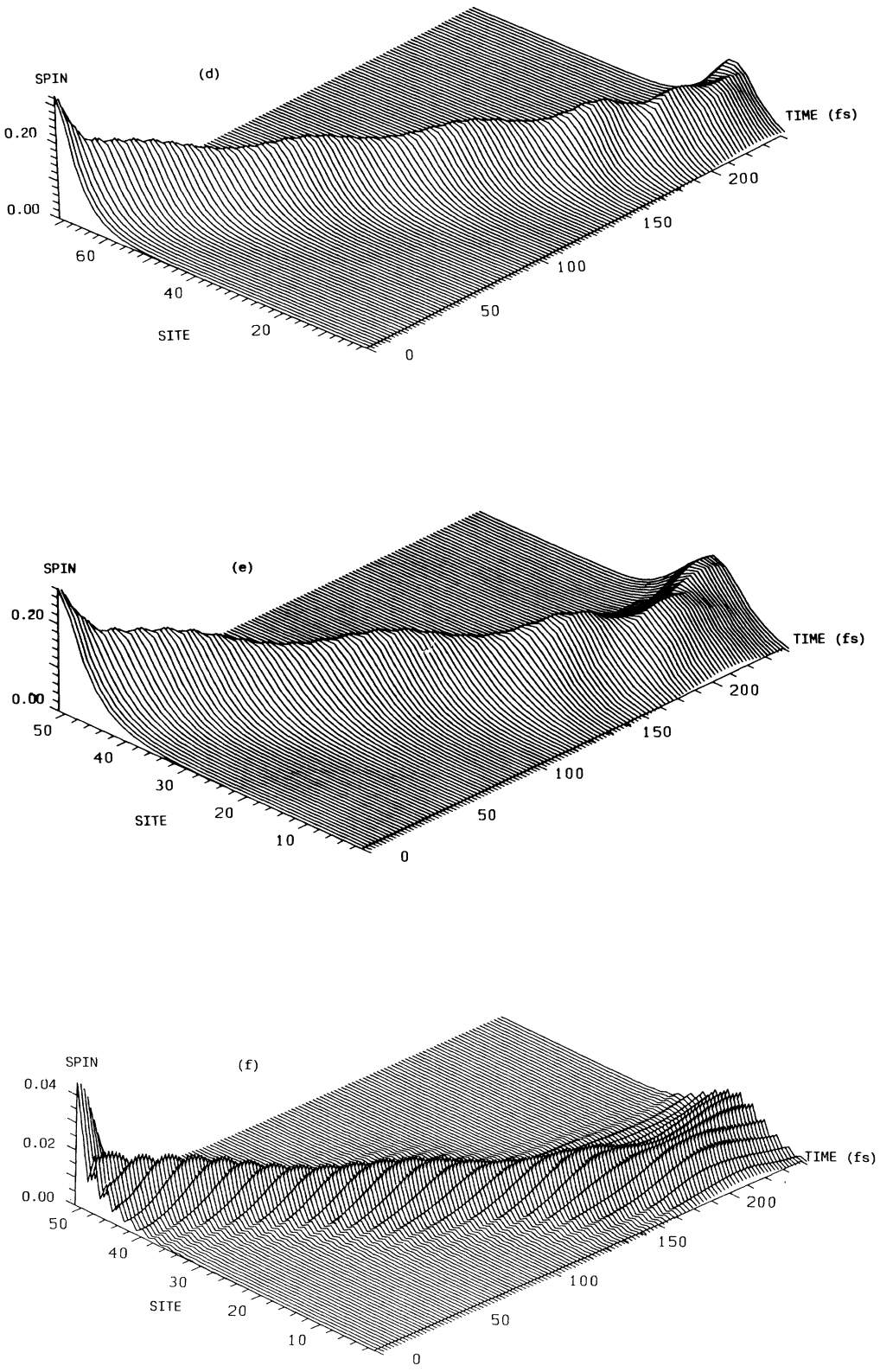

FIG. 6. (*Continued*).

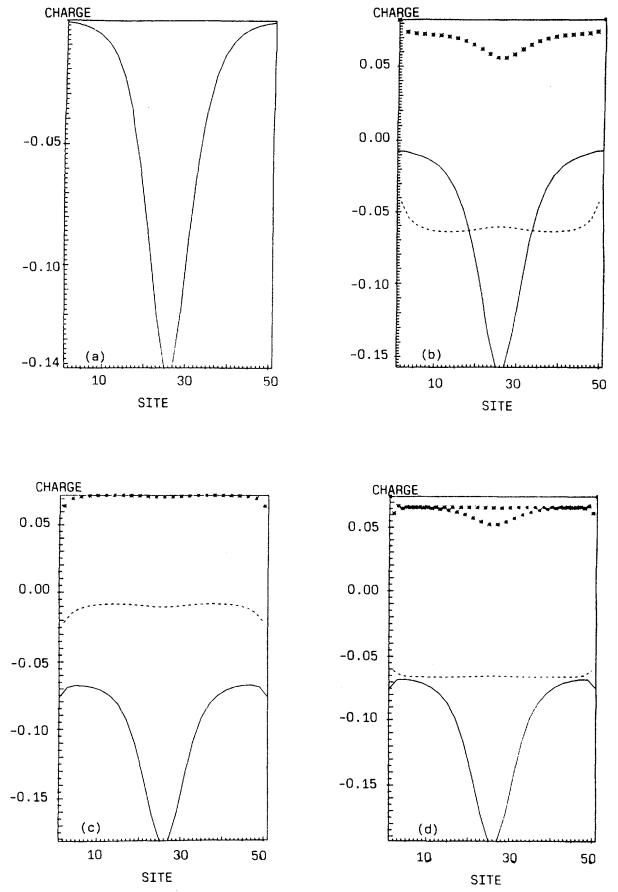

FIG. 7. Charge distribution for a negatively charged chain of 51 carbons with an optimized soliton in the middle of the chain (solid lines, odd-numbered carbons; dashed lines, even-numbered carbons; stars, oxygen). (a) No OH groups; (b) OH groups at odd-numbered carbons; (c) OH groups at even-numbered carbons; (d) OH groups at all carbons.

IV. CONCLUSION

On the basis of our *ab initio* HF CO calculations we are able to explain the experimental finding that the band gap in *t*-PA and PK is essentially the same.[15,16] We have also discussed details of the band structures. Our results are in agreement with qualitative arguments based on Hückel calculations and first-order perturbation theory. We predict that polydihydroxyacetylene should have a smaller gap than *t*-PA (10–15 %), if it could be synthesized.

From experiment it is known[15,16] that in pristine PK the concentration of unpaired spins (neutral solitons) is much smaller than in *t*-PA.[15,16] In agreement with the soliton model of conductivity, this would result in a reduced conductivity in lightly doped samples of PK as compared to *t*-PA. Although it was shown experimentally that neutral solitons most probably play no role in the mechanism of photoconductivity of *t*-PA,[32] this does not imply that in case of doping extra electrons or holes would not occupy neutral soliton levels in odd-numbered chains within the material. However, our calculations give no transport properties of the material. Further, *t*-PA samples (e.g., Naarmann) are known where lower spin concentrations are not accompanied by a reduced conductivity. In addition, the charge transport in heavily doped systems is most probably not related to solitons. Therefore, we concentrate on the properties of neutral solitons in the materials and leave the question of conductivity to future work. Our soliton simulations indicate that in PK and PDHA solitons exist that are very similar to those obtained in *t*-PA. Only quantitative changes in their properties are found. Thus we assign the experimentally found[15,16] mobile fraction of the spins in pristine PK to solitons moving freely in parts of the chains that show the enol form of the material.

From our previous calculations on *t*-PA chains containing one C=O group[12] we know that a CO group is a

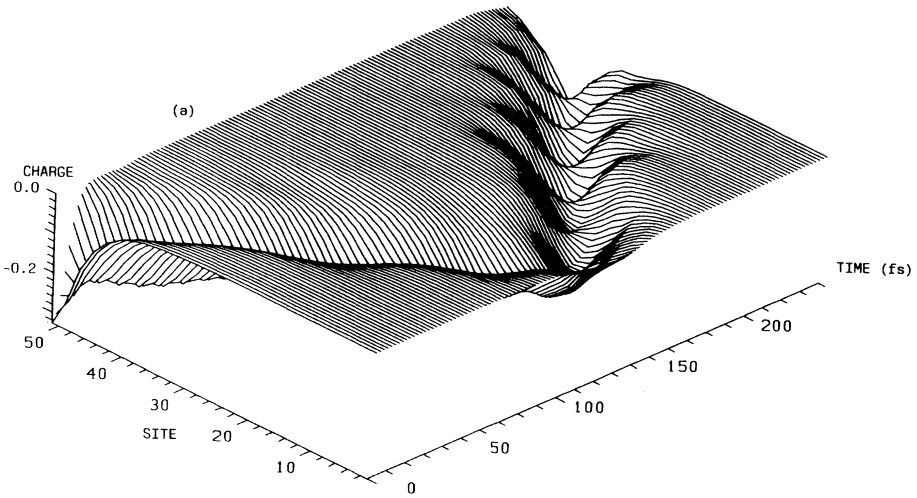

FIG. 8. Charge distribution (q_k) at odd-numbered carbons as function of site (k) and time t (in fs) for a negatively charged chain of 51 carbons. (a) No OH groups; (b) OH groups at odd-numbered carbons; (c) OH groups at even-numbered carbons; (d) OH groups at all carbons.

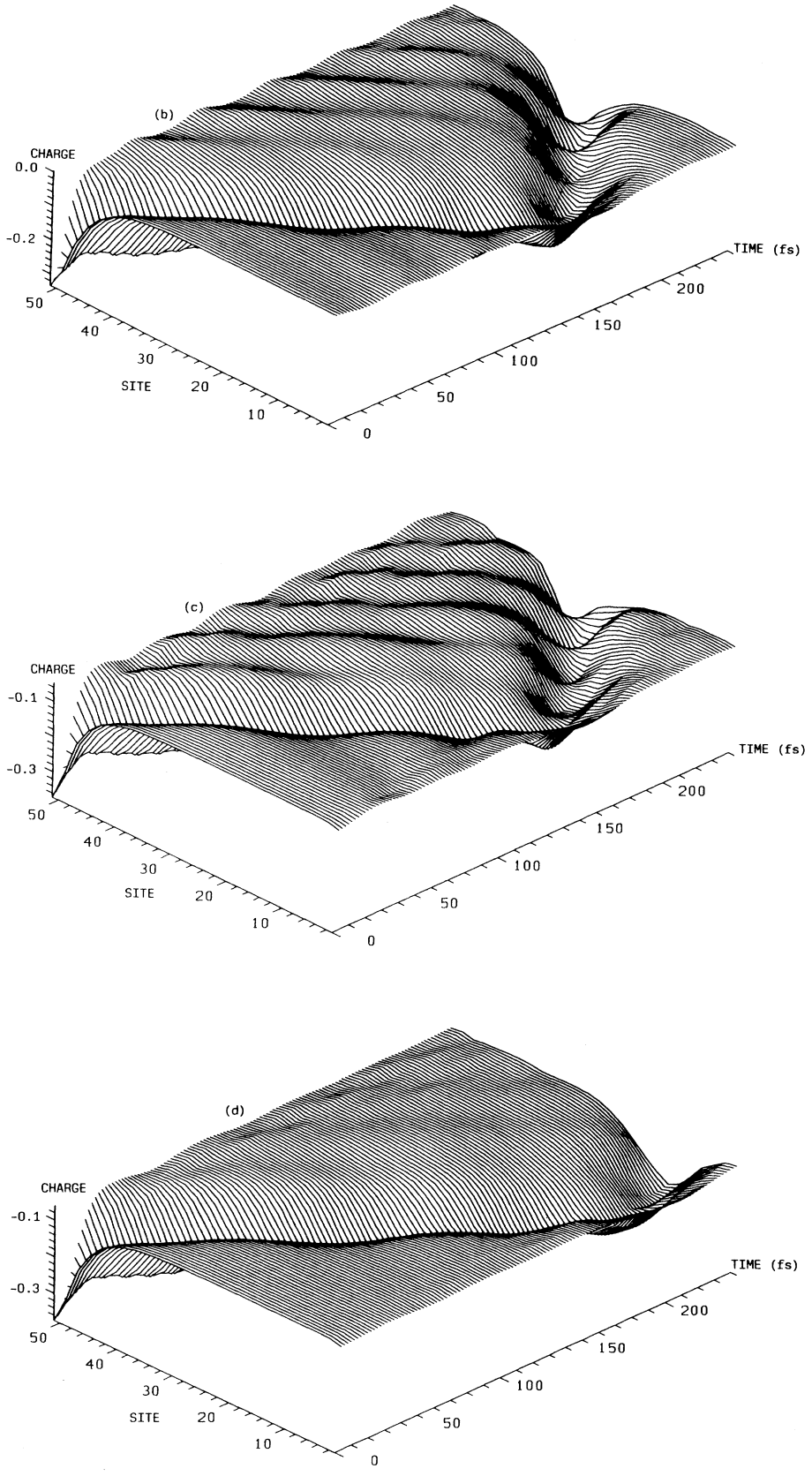

FIG. 8. (*Continued*).

trap for neutral solitons. Such a trapped soliton transfers a considerable fraction of its spin to the oxygen. Thus we assign the experimentally found localized fraction (mainly at the CO groups) of the spins in pristine PK to neutral solitons trapped at C=O groups in the material. Therefore, we could explain the basic properties of PK on the basis of *ab initio* HF CO theory and the concept of solitons within the SSH model. If we would use the Pariser-Parr-Pople model instead, we expect quantitative (width and velocities) differences in the soliton properties but no qualitative changes.[14] Thus our basic reasoning would be unchanged.

ACKNOWLEDGMENTS

We should like to express our gratitude to Professor G. Olah for calling our attention to the problem and for very interesting discussions. The financial support of the Deutsch Forschungsgemeinschaft (Project No. Ot 51/6-1) and of the Fonds der Chemischen Industrie is gratefully acknowledged.

[1]H. J. Mikeska, J. Phys. C **11**, L29 (1978).

[2]K. Maki, J. Low Temp. Phys. **41**, 327 (1980).

[3]K. J. Wahlstrand, J. Chem. Phys. **82**, 5257 (1985); K. J. Wahlstrand and P. G. Waylnes, *ibid.* **82**, 5259 (1985).

[4]S. Aubry, J. Chem. Phys. **64**, 3392 (1976); M. A. Collins, A. Blumen, J. F. Currie, and J. Ross, Phys. Rev. B **19**, 3630 (1979).

[5]A. S. Davydov and N. I. Kislukha, Phys. Status Solidi B **59**, 465 (1973); A. S. Davydov, Phys. Ser. **20**, 387 (1979); Usp. Fiz. Nauk **138**, 603 (1982) [Sov. Phys.—Usp. **25**, 898 (1982)]; *Biology and Quantum Mechanics* (Pergamon, Oxford, 1982); W. C. Kerr and P. S. Lomdahl, Phys. Rev. B **35**, 3629 (1987); A. C. Scott, Phys. Rev. A **26**, 578 (1982); Phys. Ser. **29**, 279 (1984); L. MacNeil and A. C. Scott, *ibid.* **29**, 2284 (1984); A. C. Scott, Philos. Trans. R. Soc. London Ser. A **315**, 423 (1985); P. S. Lomdahl and W. C. Kerr, Phys. Rev. Lett. **55**, 1235 (1985); A. F. Lawrence, J. C. McDaniel, D. B. Chang, B. M. Pierce, and R. K. Birge, Phys. Rev. A **33**, 1188 (1986); H. Bolterauer, *Structure, Coherence, and Chaos,* Proceedings of the MIDIT Workshop, 1986 (Manchester University, Manchester, 1986); H. Motschmann, W. Förner, and J. Ladik, J. Phys. Condens. Matter **1**, 5083 (1989); D. W. Brown, K. Lindenberg, and B. J. West, Phys. Rev. A **33**, 4104 (1986); **33**, 4110 (1986); D. W. Brown, *ibid.* **37**, 5010 (1988); D. W. Brown, K. Lindenberg, and B. J. West, Phys. Rev. B **35**, 6169 (1987); **37**, 2946 (1988); B. Mechtly and P. B. Shaw, *ibid.* **38**, 3075 (1988).

[6]J. A. Krumhansl and D. M. Alexander, in *Structure and Dynamics, Nucleic Acids and Proteins,* edited by E. Clementi and R. H. Sarma (Adenine, New York, 1983), p. 61.

[7]E. Boyland, in *Symposium on Carcinogenesis,* Proceedings of the Israel Academy of Sciences, Jerusalem, 1968, edited by E. D. Bergmann and B. Pullman (Jerusalem Academic, Jerusalem, 1969); J. Ladik, S. Suhai, and M. Seel, Int. J. Quantum. Chem. **5**, 35 (1978); J. Ladik, *ibid.* **13**, 307 (1986); A. K. Bakhshi, J. Ladik, M. Seel, and P. Otto, Chem. Phys. **108**, 223 (1986); K. Laki and J. Ladik, Int. J. Quantum Chem. **3**, 51 (1976); F. Beleznay, S. Suhai, and J. Ladik, *ibid.* **20**, 683 (1981).

[8]J. Ladik and J. Cizek, Int. J. Quantum Chem. **26**, 955 (1984); J. Ladik, in *Molecular Basis of Cancer, Part A,* edited by R. Rein (Liss, New York, 1985), p. 343.

[9]D. Hofmann, W. Förner, and J. Ladik, Phys. Rev. A **37**, 4429 (1988); W. Förner, *ibid.* **38**, 939 (1988); **40**, 6438 (1989); W. Förner, J. Ladik, P. Otto, and F. Martino, *ibid.* **40**, 6457 (1989).

[10]W. P. Su, J. R. Schrieffer, and A. J. Heeger, Phys. Rev. Lett. **42**, 1698 (1979); W. P. Su, Solid State Commun. **35**, 899 (1980); W. P. Su, J. R. Schrieffer, and A. J. Heeger, Phys. Rev. B **22**, 2099 (1980); **28**, 1138(E) (1983).

[11]A. Godzik, M. Seel, W. Förner, and J. Ladik, Solid State Commun. **60**, 609 (1987); C.-M. Liegener, W. Förner, and J. Ladik, *ibid.* **61**, 203 (1987); S. R. Phillpot, D. Baeriswyl, A. R. Bishop, and P. S. Lomdahl, Phys. Rev. B **35**, 7533 (1987).

[12]W. Förner, M. Seel, and J. Ladik, Solid State Commun. **57**, 463 (1986); J. Chem. Phys. **84**, 5910 (1986).

[13]S. Kivelson and D. E. Heim, Phys. Rev. B **26**, 4278 (1982); A. J. Heeger and J. R. Schrieffer, Solid State Commun. **48**, 207 (1983); Z. G. Soos and S. Ramashesha, Phys. Rev. Lett. **51**, 2374 (1983); H. Sasai and H. Fukutome, Synth. Met. **9**, 295 (1984); W. P. Su, Phys. Rev. B **34**, 2988 (1986); S. Kivelson and Wei-kang Wu, *ibid.* **34**, 5423 (1986).

[14]C. L. Wang and F. Martino, Phys. Rev. B **34**, 5540 (1986); W. Förner, C. L. Wang, F. Martino, and J. Ladik, *ibid.* **37**, 4567 (1988); R. Markus, W. Förner, and J. Ladik, *ibid.* **63**, 135 (1988); H. Orendi, W. Förner, and J. Ladik, Chem. Phys. Lett. **150**, 113 (1988).

[15]G. A. Olah, E. Zadok, R. Edler, D. H. Adamson, W. Kasha, and G. K. Surya Prakash, J. Am. Chem. Soc. **111**, 9123 (1989).

[16]K. C. Khemani and F. Wudl, J. Am. Chem. Soc. **111**, 9124 (1989).

[17]G. Del Re, J. Ladik, and G. Biczó, Phys. Rev. **155**, 997 (1967); J.-M: André, L. Gouverneur, and G. Leroy, Int. J. Quantum Chem. **1**, 427 (1967); **1**, 451 (1967); J. Ladik, *Quantum Theory of Polymers as Solids* (Plenum, New York, 1988).

[18]P. Otto (unpublished).

[19]L. Gianolio, R. Pavoni, and E. Clementi, Gazz. Chim. Ital. **108**, 181 (1978).

[20]L. Gianolio and E. Clementi, Gazz. Chim. Ital. **110**, 179 (1980).

[21](a) A. K. Bakhshi and J. Ladik, Solid State Commun. **60**, 316 (1986); **61**, 71 (1987); **65**, 1203 (1988); P. Otto and J. Ladik, Synth. Met. **36**, 327 (1990); (b) A. K. Bakhshi, J. Ladik, and M. Seel, Phys. Rev. B **35**, 704 (1987).

[22]J. Ladik, *Quantum Theory of Polymers as Solids* (Plenum, New York, 1988).

[23]C. R. Fincher, Jr., C.-E. Chen, A. J. Heeger, A. G. MacDiarmid, and J. B. Hastings, Phys. Rev. Lett. **48**, 100 (1982).

[24]D. Vanderbilt and E. J. Mele, Phys. Rev. B **22**, 3939 (1980).

[25]A. J. Streitwieser, *Molecular Orbital Theory for Organic Chemists* (Wiley, New York, 1961).

[26]W. P. Su and J. R. Schrieffer, Proc. Natl. Acad. Sci. U.S.A. **77**, 5626 (1980); F. Guinea, Phys. Rev. B **30**, 1884 (1984); A. R. Biship, D. K. Campbell, P. S. Lomdahl, B. Horowitz, and S. R. Phillpot, Phys. Rev. Lett. **52**, 671 (1984).

[27]W. Förner, Solid State Commun. **63**, 941 (1987).
[28]R. S. Mulliken, J. Chem. Phys. **23**, 1833 (1955).
[29]S. Suhai, Phys. Rev. B **27**, 3506 (1983).
[30]C.-M. Liegener, J. Chem. Phys. **88**, 6999 (1988).
[31]W. Förner, Synth. Met. **30**, 135 (1989).
[32]M. Sinclair, D. Moses, R. H. Friend, and A. J. Heeger, Phys. Rev. B **36**, 4296 (1987); N. F. Colaneri, R. H. Friend, H. E. Schaffer, and A. J. Heeger, *ibid.* **38**, 3960 (1988); P. D. Townsend and R. H. Friend, *ibid.* **40**, 3112 (1989).